Influence of Environmental Factors on Pesticide Adsorption by Black Carbon: pH and Model Dissolved Organic Matter

5 AUTHORS, INCLUDING:

Xiaoyu Xiao

4 PUBLICATIONS **60** CITATIONS

SEE PROFILE

Influence of Environmental Factors on Pesticide Adsorption by Black Carbon: pH and Model Dissolved Organic Matter

YUPING QIU,[†] XIAOYU XIAO,[†]
HAIYAN CHENG,[‡] ZUNLONG ZHOU,[†] AND
G. DANIEL SHENG*,[†]

College of Biological and Environmental Engineering, Zhejiang University of Technology, Hangzhou 310032, China, and Department of Environmental Science and Technology, East China Normal University, Shanghai 200062, China

Loading two organic acids of known molecular structures onto a black carbon was conducted to study the influence of pH and dissolved organic matter on the adsorption of pesticides. Tannic acid at the loading rates of 100 and 300 μmol/g reduced the surface area of black carbon by 18 and 63%, respectively. This was due principally to the blockage of micropores, as verified by measured pore volumes and pore-size distributions. With a comparatively much smaller molecular structure, gallic acid did not apparently influence these properties. The intrinsic acidities of the two acids increased the surface acidity from 1.88 mmol/g of black carbon to 1.93–2.02 mmol/g after DOM loading, resulting in a reduction in isoelectric point pH from 1.93 to 1.66–1.82. The adsorption of propanil, 2,4-D and prometon by black carbon free and loaded of DOM was dependent on pH because major adsorptive forces were the interactions between neutral pesticide molecules and uncharged carbon surfaces. The adsorption was diminished considerably by the deprotonation of 2,4-D and protonation of prometon, as well as the surface charge change of black carbon. Tannic acid of 100 and 300 μmol/g on black carbon reduced the pesticide adsorption at the equilibrium concentration of 10 mg/L by an average of 46 and 81%, respectively, consistent with the reductions of 42 and 81% in micropore volume. At the equilibrium concentration of 30 mg/L, the mesopore surface became the additional adsorptive domain for propanil. Loading tannic acid made the mesopore surface less accessible, due presumably to the enhanced obstruction by tannic acid.

Introduction

Increased biomass burning and fossil fuel consumption during the past decades have drastically increased the input of black carbon (BC) into the environment (*1*). Global emission of BC into the atmosphere is estimated to exceed 0.5–2.6 hundred million tons per year (*2*). Most of the emitted BC subsides and eventually enriches in soils and sediments (*3*). Extrinsic BC arising from burns of organic precursors

has been identified as potential "supersorbents" for synthetic organic compounds (SOCs) in soils and sediments (*4–8*).

Adsorption of SOCs by BC is influenced by pH and dissolved organic matter (DOM). The pH influence is connected to two aspects, the surface properties of BC and the speciation of SOCs. The former is characterized primarily by surface functionality. Chun et al. (*9*) reported a higher surface acidity of BC as compared to activated carbon (AC) because of much more abundant acidic groups (e.g., —OH and —COOH) on BC surfaces. Such hydrophilic groups act as water adsorption sites and, in the presence of water, effectively obstruct the surface accessible otherwise to SOCs (*10*). Depending on pH, the protonation and deprotonation of functional groups results in a different net charge on the BC surfaces (*11*). Protonation or deprotonation of a dissociable SOC is similarly determined by pH. Yang et al. (*10*) found that reduced bromoxynil adsorption on BC at pH > pK_a (=4.06) was due mainly to the deprotonation of the hydroxyl of the molecule. Similarly, reduced ametryne adsorption at pH < pK_a (=4.10) was ascribed to the protonation of the amine groups of the molecule.

New evidence presents the fact that the surface and sorptive activities of a BC are attenuated by DOM (*12, 13*). Considering that the background concentrations of DOM are tens-to-thousands of times higher than those of SOCs in soil–water environments, preloading DOM onto BC rather than measuring the competitive adsorption in a DOM–SOC system seems more plausible to investigate the effect of DOM on SOC adsorption (*14*). Reduced diuron sorption on aged wheat char and char-amended soil was attributed to the adsorption of DOM on the char (*15*). The aging of char in soil prior to SOC sorption implies that DOM was preloaded on the surface of the char, thereby covering adsorptive sites and blocking pores (*16*). Similar work has been conducted using AC and activated carbon fiber (ACF) (*17–22*), in which the main focus was placed on the influence of the pore size distributions of AC and ACF. In most cases, soil DOM, humic acid and/or fulvic acid were chosen as model DOM molecules, whose structures and molecular weights (MWs) are not clearly defined (*13, 23–25*).

The influence of DOM on BC surface area and porosity and thus SOC adsorption may be understood using model DOM with a clearly defined molecular structure and exact loadings. As DOM, along with BC and many SOCs, contains an abundance of pH-dependent functional groups, the influence of pH must be taken into consideration. The objective of this study was thus to determine the influence of loaded model DOM on pesticide adsorption by BC at various pH values. A BC generated from crop residues was used. Three pesticides (propanil, 2,4-dichlorophenoxic acid (2,4-D) and prometon) tested have similar MWs but differ in their protonation and deprotonation properties. Two model DOM materials (tannic acid (TA) and gallic acid (GA)), the MW of the former being exactly 10 times that of the latter, were chosen to be loaded onto the surface of BC at various rates prior to pesticide adsorption.
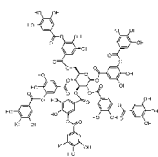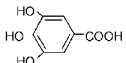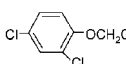
Experimental Section
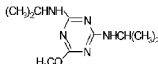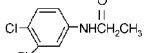
Materials. TA (purity of >95%) and GA (>95%) were obtained from Shanghai Chemical Reagents Company (Shanghai, China) and used as received. Propanil (>98%), 2,4-D (>95%) and prometon (>98%) were purchased from Sigma-Aldrich (Shanghai, China). Selected physicochemical properties of these compounds are listed in Table 1. Based on their Henry's Law constants, all three pesticides are nonvolatile. Rice straw (*Oryza sativa* L.) was collected from a farmland in Taizhou,

* Corresponding author phone: +86-571-88320243; fax: +86-571-88320884; e-mail: dansheng@zjut.edu.cn.
† Zhejiang University of Technology.
‡ East China Normal University.

TABLE 1. Selected Physicochemical Properties of Model DOMs and Pesticides at 25 °C[a]

DOM and Pesticide	Structure	MW (g/mol)	S_w (mg/l)	ρ (g/cm^3)	pK_a	K_H (atm-m^3/mol)	$\log K_{ow}$
TA		1701.2	2.50×10^{5} [b]	/	/	-	-1.19 [c]
GA		170.12	1.19×10^{4} (20°C)	/	3.13 (20°C)	1.22×10^{-19}	0.70
2,4-D		221.04	677	1.420	2.87	1.02×10^{-8}	2.81
Prometon		225.29	750	1.088	4.3 [d]	1.98×10^{-9}	2.99
Propanil		218.08	225	1.054	/	4.50×10^{-9}	3.07

[a] Model DOMs: Tannic acid (TA) and gallic acid (GA); MW: molecular weight; S_w: aqueous solubility; ρ: density of pesticide; pK_a: negative log-transformed acid dissociation constant; K_H: Henry's Law Constant; $\log K_{ow}$: negative log-transformed octanol−water partition coefficient; data from ref *26* unless otherwise indicated. [b] From http://www.chemblink.com/products/1401-55-4C.htm. [c] From ref *27*. [d] From ref *28*.

China. After air-drying for one week, 10 kg of rice straw was burned in an open field under local weather conditions (a clear windless afternoon of December, temperature ~15 °C, relative humidity ~25%). The char of ~250 g obtained was suspended and shaken in 1 L of 1 mol/L HCl solution four times and subsequently in 1 L of HCl−HF solution (1 mol/L−1 mol/L) six times for demineralization to remove silica and metal oxides. Following thorough washing with distilled water six times to neutral pH, the residue was dried at 80 °C to obtain a rice-straw-derived BC. Elemental analysis indicated that the C content of BC was ~80% and C+H+O accounted for ~92% of BC mass.

TA and GA Loading. Prior to loading TA and GA, their adsorption isotherms by BC were determined. TA or GA (50 mL) with a range of initial concentrations (200−1400 μmol/L) prepared in 0.01 mol/L NaCl (to maintain a constant ionic strength) and 1.5 mmol/L NaN$_3$ (a biocide) solution were introduced into a series of 100 mL flasks containing 0.050−0.080 g BC. The flasks were capped and agitated for 2 weeks at 25 °C. TA and GA in solution phases were then analyzed by HPLC (Supporting Information (SI) Figure S1). The amounts of TA and GA adsorbed on BC were calculated by difference. The isotherms were constructed by plotting the amounts adsorbed versus the corresponding equilibrium concentrations (SI Figure S2). These isotherms were well fitted to the Freundlich equation. To load TA and GA onto BC at loading rates of 100 and 300 μmol/g, the obtained Freundlich parameters were used to calculate the initial concentrations of TA and GA required at the solid/liquid ratios used. TA (276 and 840 μmol/L) and GA (421 and 1286 μmol/L) solutions were then prepared to load the two acids onto BC. The equilibrated suspensions were filtered. The solids were washed with distilled water four times and subsequently vacuum-dried for a week at 80 °C. Losses of TA and GA during rinse were negligible as verified by HPLC. The DOM-loaded BC samples were designated as 100TA-BC, 300TA-BC, 100GA-BC, and 300GA-BC, respectively, where 100 and 300 indicate the respective loadings.

Characterization of BC Samples. BC samples free and loaded of DOM were measured for their Brunauer−Emmett−Teller (BET) surface areas (S_{BET}) and pore size distributions from N$_2$ adsorption at 77 K using a Micromeritics ASAP-2010 surface area analyzer (Micromeritics Instrument Corp., Norcross, GA). The Horvath−Kawazoe (HK) and Barrett−Joyner−Halendar (BJH) theories were used to analyze the micropore and mesopore distributions, respectively (*29, 30*). The amphoteric properties of BC samples (surface acidity/basicity) were evaluated by the selective acid/base neutralization method (*31*). The method assumes that HCl neutralizes all basic groups, NaOH neutralizes all acidic groups (carboxyls, lactones, and phenolic hydroxyls), Na$_2$CO$_3$ neutralizes carboxyls and lactones, and NaHCO$_3$ neutralizes carboxyls only. The zeta potentials at various pH values were measured by the laser Doppler electrophoresis technique using a Zetamaster potentiometer (Malvern Instruments, UK) (*32*). The pH of isoelectric point (pH$_{IEP}$), at which the net surface charge is zero, was obtained.

Pesticide Adsorption. The pesticide adsorption was determined in a series of 100 mL flasks containing appropriate masses of BC samples and 50 mL of aqueous solutions. The solutions of different initial pesticide concentrations (10−60 mg/L) were obtained by mixing appropriate volumes of pesticide stock solutions and distilled water containing 1.5 mmol/L NaN$_3$ and 0.01 mol/L NaCl. Solid-to-solution ratios were properly selected to have 30−80% solute adsorbed at equilibrium. The solution pH was then adjusted to two desired values with 0.01 mol/L HCl or 0.01 mol/L NaOH. The flasks were agitated at ~25 °C on an incubation shaker at 125 rpm for 48 h. Pretests indicated that pesticide adsorption reached an apparent equilibrium within 30 h (SI Figure S3). Samples were then filtered with Whatman grade 5 filter paper (Shanghai, China). The concentrations of pesticides in filtrates were analyzed by HPLC equipped with a C-18 μ column and a dual λ absorbance detector (Waters Corp., Milford, MA) at the wavelength of 252, 220, and 230 nm for propanil, 2,4-D and prometon, respectively. The mobile phase was the aqueous solution of 60% acetonitrile for propanil, 90% methanol for 2,4-D, and 75% methanol for prometon. The amounts adsorbed were calculated from the difference between the initial and equilibrium concentrations. All the

TABLE 2. Selected Physicochemical Properties of BC Samples

| | | pore structure | | | | surface characteristics | | | | | |
| | | (nm) | | (cm³/g) | | (mmol/g) | | | | | |
sample	S_{BET} (m²/g)	$d_{total}{}^{a}$	$d_{micro}{}^{b}$	$V_{total}{}^{c}$	$V_{micro}{}^{d}$	carboxyl	lactone	phenolic hydroxyl	total acid	base	pH_{IEP}
BC	1085	6.00	1.12	1.63	0.26	0.99	0.79	0.10	1.88	0.25	1.93
100TA-BC	893	6.32	1.20	1.41	0.15	0.94	0.88	0.16	1.98	0.17	1.71
300TA-BC	402	7.30	1.26	0.73	0.05	0.89	0.93	0.20	2.02	0.14	1.66
100GA-BC	1067	6.02	1.13	1.63	0.23	0.99	0.82	0.12	1.93	0.22	1.82
300GA-BC	1048	6.08	1.14	1.62	0.22	0.96	0.87	0.14	1.97	0.18	1.72

[a] Average total pore width (4 V/A by BET). [b] Horvath−Kawazoe median pore width ($0.75 \leq d < 2$ nm). [c] Single point adsorption total pore volume of pores less than 81.4 nm in diameter at $P/P_o = 0.97$. [d] Horvath−Kawazoe cumulative pore volume between 0.75−2.0 nm.

measurements were performed in duplicate; average values are reported. Blank samples not containing BC were also prepared and losses of pesticides in solution phases other than adsorption were negligible. The equilibrium pH values of the filtrates were measured to be 1.25 ± 0.03 and 5.90 ± 0.07, respectively.

Results and Discussion

Characterization of BC and DOM-Loaded BC Samples. The BET surface area (S_{BET}) of BC was 1085 m²/g (Table 2), which was larger than the previously reported data (2−776 m²/g) (*1, 4*), due likely to the differences in precursors, burning conditions, and purification process (*33*). The S_{BET} was in the range of those for activated carbon, indicating the effectiveness of burning in creating the carbon surface and porous structure.

Careful examination indicates that loading TA to BC generated a more profound influence than loading GA on the surface properties of the BC. When TA was loaded, the S_{BET} of BC decreased to 893 and 402 m²/g at the loading rates of 100 and 300 μmol/g, respectively, corresponding to 18% (=(1085−893)/1085 × 100%, similarly calculated hereafter) and 63% reductions. The same decreasing order was also observed in total pore volume (V_{total}) that it decreased from 1.63 to 1.41 and 0.73 cm³/g at the two TA loading rates, respectively, or 13 and 55% reductions. Similarly, the micropore volume (V_{micro}, pore diameter <2.0 nm) of TA-loaded BC samples decreased from 0.26 to 0.15 and 0.05 cm³/g, respectively. The corresponding percentages of reduction in V_{micro} being 42 and 81%, respectively, were higher than those in S_{BET} and V_{total}, indicating the blockage of mainly micropores by TA. This is also supported by the average pore width, d_{total}, that it increased with TA loading rate. By comparison, loading GA resulted in little changes in all the above respects. This appeared to result from the much smaller molecular size of GA as compared to TA.

Consistent results can also be derived from the HK and BJH pore size distributions of BC samples (Figure 1). BC possessed the dominant pore width of ∼0.8 nm within the micropore range (diameter <2.0 nm) and of ∼3.5 nm within the mesopore range (diameters of 2.0−50 nm). Both 100GA-BC and 300GA-BC showed similar pore size distributions with peaks of similar intensities at the same pore width, indicating that GA did not effectively block the pores of BC. For 100TA-BC and 300TA-BC within the micropore range, the maximum peak intensities were reduced to 0.176 and 0.006 cm³/g/nm (Figure 1a), respectively, indicating that TA effectively blocked the micropores of BC. The maximum peak positions also moved to larger pore width, consistent with the d_{micro} (Table 2). Within the mesopore range, on the other hand, the maximum peak intensity of 100TA-BC had little change and that of 300TA-BC was reduced by about half (Figure 1b), as compared to BC, suggesting that mesopores were less effectively blocked by TA. The reductions in V_{total} of 100TA-BC (13%) and 300TA-BC (55%) in comparison to
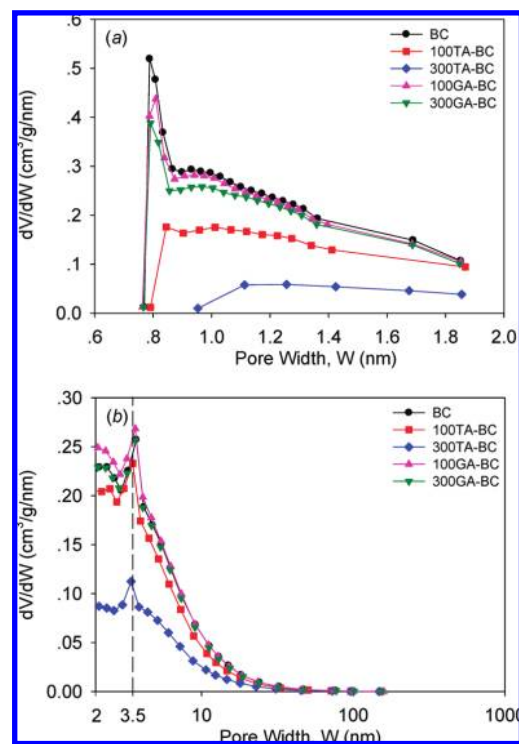

FIGURE 1. Pore-size distributions of BC and model DOM-loaded BC samples: (a) micropore plots by HK method, (b) mesopore plots by BJH method.

BC being similar to those in maximum peak intensity over the mesopore range implies that the mesopore blockage by TA contributed mainly to the decrease in total volume of BC.

The elemental analysis showed that BC had high contents of H (2.02%, w/w) and O (9.05%, w/w), suggesting its abundant oxygen-containing surface functional groups. Table 2 shows that the carboxyls, lactones and phenolic hydroxyls on BC were 0.99, 0.79, and 0.10 mmol/g, respectively, and that the total acidity was 7.5 times higher than the basicity. Loading TA and GA increased the total acidity of BC, due apparently to the abundant phenolic hydroxyls in the molecular structures of the two acids. This is manifested in Table 2 that loading TA and GA resulted in larger increases in the numbers of phenolic and lactonic groups than the decreases in the numbers of carboxyl and basic groups, although the number of total functional groups (total acid + base) remained rather invariant (2.14 ± 0.02 mmol/g).

The zeta potential (ζ) results mainly from the protonation and deprotonation of surface functional groups, which forms an electrical double layer (*34*). SI Figure S4 shows the change in zeta potentials of BC samples as a function of solution pH. These zeta potentials decreased monotonically with increasing solution pH. The isoelectric point, pH_{IEP}, is the pH at
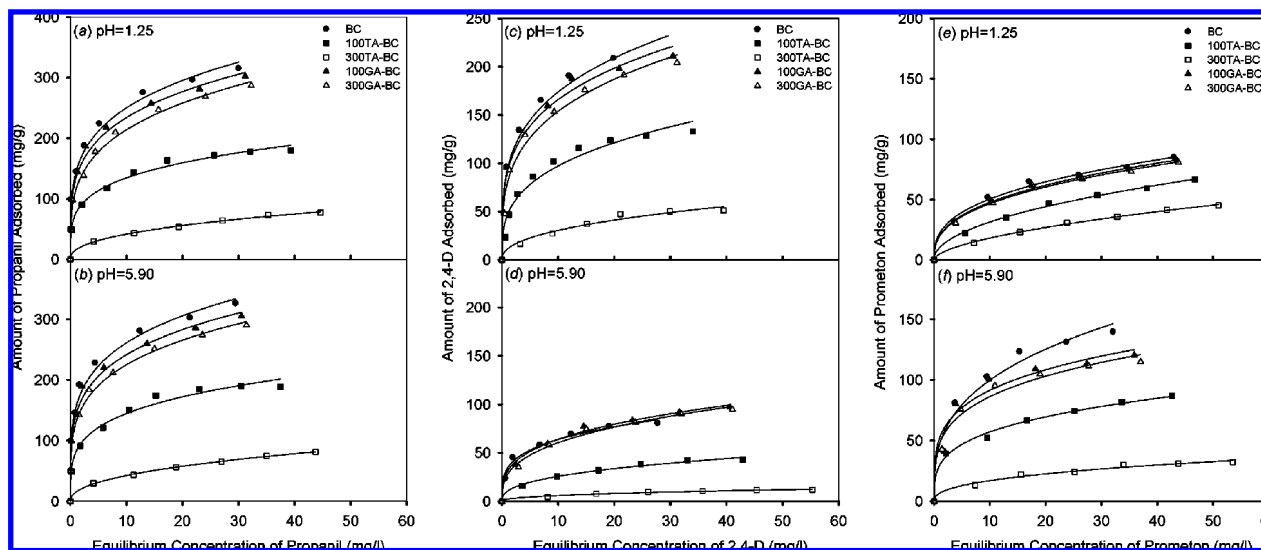
FIGURE 2. Adsorption of propanil (a,b), 2,4-D (c,d) and prometon (e,f) by BC samples at two experimental pH values: 1.25 ± 0.03 and 5.90 ± 0.07.

which the zeta potential on BC surfaces is zero. Loading TA and GA decreased the pH_{IEP} of BC, due apparently to the intrinsic acidities of the two acids. Larger decreases in pH_{IEP} by TA (0.22 and 0.27 pH unit, respectively) than by GA (0.11 and 0.21 pH unit) were consistent with the higher acidity of the former acid than that of the latter and with the Boehm titration (Table 2).

Adsorption of Pesticides on BCs as Influenced by pH. The adsorption isotherms of pesticides on BC samples from aqueous solutions at two pH values are shown in Figure 2. These isotherms were fitted well to the following Freundlich equation:

$$q_e = K_F C_e^n$$

where q_e and C_e are equilibrium concentrations of a pesticide on a BC and in solution, respectively, K_F is the Freundlich affinity coefficient, and n (unitless) indicates the nonlinearity of an isotherm (35). The fitted curves are drawn in Figure 2 to assist in visualization.

A change in solution pH may influence not only the zeta potential of BC but also the charge properties of ionizable pesticides (10). In this work, the pH_{IEP} of all BC samples fell between the two experimental pH values (pH 1.25 and 5.90), indicating a net charge reversal at the two pH values. The pK_a values of 2,4-D and prometon (Table 1) are also between the two experimental pH values, indicating that the two pesticides were present predominantly in molecular or ionic forms at the two pH values.

Propanil, a neutral pesticide, was adsorbed by BC samples in the decreasing order of BC > 100GA-BC > 300GA-BC > 100TA-GC > 300TA-GC (Figures 2a and b). This order was consistent with the measured surface areas of these samples, suggesting that the surface area was the controlling adsorptive factor for neutral pesticides over the surface functionality of BC. In fact, normalization to surface area gives nearly superimposable isotherms for BC, 100GA-BC and 300GA-BC. Slightly lower normalized isotherms for 100TA-BC and 300TA-BC manifested minor effects of the surface functionality, due most likely to the larger molecular size of TA with an abundance of phenolic hydroxyls. As pointed out by Wang and Xing (36), the structure of BC is constituted of short stacks of graphene sheets arranged in a disordered fashion. It is thus presumed that propanil was adsorbed on BC primarily via the London (dispersive) forces, which was further enhanced by the $\pi-\pi$ interactions between propanil

molecules and the uncharged graphene sheets of BC. Such a mechanism for aromatics adsorption by BC has been reported in the literature (37, 38). For a given sorbent, on the other hand, the propanil adsorption at the two experimental pHs was quite similar in magnitude over the experimental concentration range (Figure 2a and b). This is evidenced by both K_F and n values for propanil adsorption being virtually independent of solution pH (SI Table S1). Considering that the opposite net charge existed on the BC surfaces at the two pH values, propanil was apparently adsorbed mostly on the uncharged surfaces of BC samples. Polar functional groups preferentially adsorbed water and hence reduced propanil adsorption.

Adsorption of 2,4-D was much lower at pH 5.90 than at pH 1.25 (Figure 2c and d), as indicated by similar n but different K_F values for a given BC (SI Table S1). This suggests differential intensities of intermolecular interactions between 2,4-D and BC at the experimental pH values higher and lower than the pK_a of 2,4-D as well as the pH_{IEP} of BC. With a pK_a of 2.87, 2,4-D is present in solution in 99.9% anionic form at pH 5.90 (by calculation) due to the deprotonation of —COOH, and in 97.6% molecular form at pH 1.25. According to the propanil adsorption, higher 2,4-D adsorption at pH 1.25 was attributed to the interactions between 2,4-D molecules and the uncharged BC surfaces. Reduced 2,4-D adsorption at pH 5.90 was due obviously to the dissociation of 2,4-D. Much weaker interactions between graphene sheets and ionic species and the electrical repulsion between the negative zeta potential (electric charge) and 2,4-D anions may have together contributed to the reduced 2,4-D adsorption at this pH.

The adsorption of prometon by BC was in direct contrast to that of 2,4-D in terms of pH-dependency. Prometon was adsorbed more at pH 5.90 than at pH 1.25 (Figure 2e and f). Similar calculations showed that prometon is present in solution as a 99.9% cationic species at pH 1.25 because of the protonation of isopropylamine, and as a 97.5% molecular species at pH 5.90. The higher adsorption of prometon at pH 5.90 was once again attributed largely to the interactions between prometon molecules and the uncharged BC surfaces.

Adsorption of Pesticides on BCs as Influenced by Model DOMs. Following a week of drying, TA and GA were strongly loaded on BC that they were not desorbed or displaced to any significant extent by pesticides during adsorption (SI Figure S1d and e). Preloaded compounds being difficult to desorb from carbon materials has been reported in the

TABLE 3. Adsorption (q_{10}) and Percent Reduction in Adsorption (q_{10}%) of Pesticides at Equilibrium Concentration of 10 mg/L on BCs

pH	pesticide	q_{10} (mg/g)					q_{10}%			
		BC	100TA-BC	300TA-BC	100GA-BC	300GA-BC	100TA-BC	300TA-BC	100GA-BC	300GA-BC
1.25	propanil	250.5	134.6	41.6	234.3	214.1	46.3	83.4	6.5	14.5
	2,4-D	174.2	97.4	30.6	166.0	154.0	44.1	82.4	4.7	11.6
	prometon	50.4	31.3	18.1	47.6	46.6	37.9	64.1	5.6	7.5
5.90	propanil	261.0	144.6	42.3	241.4	224.8	44.6	83.8	7.5	13.9
	2,4-D	64.0	25.7	6.1	63.8	60.4	59.8	90.5	0.3	5.6
	prometon	99.8	57.1	17.1	91.5	86.4	42.8	82.9	8.3	13.4

literature (e.g., ref *39*). It was found that adsorption occurred in adsorbent pores larger than 1.7 times adsorbate molecule's second widest dimension (*40*). Based on their average diameter of 1.6 nm (*41*), TA molecules are considered inaccessible to pores with a diameter smaller than 2.72 nm and thus possibly block the micropores and the lower end of mesopores. GA has a molecular diameter of 0.57 nm as calculated by Gaussian98 software (*42*), and can thus block an insignificant portion of the micropores of BC. These analyses are supported by the measured pore size distributions (Table 2 and Figure 1) and also consistent with the measured pesticide adsorption (Figure 2). The following discussion is therefore limited to the cases of loading TA because of the little influence of GA.

We first analyze the adsorption data to determine the adsorptive domains for pesticides. For porous materials, physisorption in micropores occurs via a pore-filling process, whereas in mesopores it occurs through monolayer-multilayer adsorption followed by capillary condensation (*43*). The former (in micropores) was believed to occur prior to the latter, due possibly to the differences in adsorptive potential (*44*). Although loading TA significantly reduced, in particular, the micropore volume of BC (Table 2 and Figure 1), the remaining micropores played yet presumably a significant role in pesticide adsorption. To analyze on a more comparative basis the role of the micropores, the adsorption (q_{10}) at the equilibrium concentration of 10 mg/L and the corresponding percent reduction in adsorption (q_{10}%) are obtained (Table 3). Consider, for example, the cases of propanil adsorption at pH 1.25 by BC, 100TA-BC and 300TA-BC where these adsorbents had micropore volumes (V_{micro}) of 0.26, 0.15, and 0.05 cm³/g, respectively. Assuming the micropores of these adsorbents were completely filled by propanil with a density (ρ) of 1.054 g/cm³ at 25 °C, the calculated amounts of propanil on BC, 100TA-BC and 300TA-BC due to micropore-filling only are 274 ($=V_{micro} \times \rho \times 10^3/MW = 0.26$ cm³/g × 1.054 g/cm³ × 10³), 158 and 53 mg/g, respectively. These numbers are larger than the corresponding q_{10} values, manifesting that these BC samples provided sufficient micropores for propanil adsorption at low equilibrium concentrations.

We now evaluate the influence of loading TA on the reduction in pesticide adsorption by BC samples at low equilibrium concentrations. The calculated percent reduction in adsorption (q_{10}%) shows that the adsorption of each pesticide by 100TA-BC and 300TA-BC, as compared to by BC, decreased by 37.9−59.8% and 64.1−90.5%, respectively, with the average reductions being 46 and 81%. The reductions in the micropore volumes of 100TA-BC and 300TA-BC, as compared to BC, were 42% (=(0.26−0.15)/0.26 × 100%) and 81% (=(0.26−0.05)/0.26 × 100%), respectively. The two reductions, i.e., the reduction in pesticide adsorption and that in micropore volume, for a given BC being similar demonstrates that the reduced pesticide adsorption by TA-loaded BC was due primarily to the reduced microporosity of BC at low pesticide concentrations. Our finding here is in well agreement with other studies (e.g., ref *23*).

We further examine the influence of loading TA on pesticide adsorption by BC at comparatively higher equilibrium concentrations. As the pesticide concentration increases to a certain level, the micropores of BC are expected to become fully filled and thereafter the mesopores provide additional adsorptive domains for pesticides. From the determined mesopore size distributions (2.0−50.0 nm), loading TA (300 μmol/g) reduced the mesopore surface area from 842 m²/g of BC to 359 m²/g of 300TA-BC, a 57% reduction. SI Table S2 lists the pesticide adsorption (q_{30}, cm³/g) by BC and 300TA-BC at the pesticide equilibrium concentration of 30 mg/L. Only those of propanil exceeded the micropore volumes of respective BC samples. By subtracting the micropore volumes from the respective adsorptions, the remainders are considered to be the propanil adsorption in the mesopores. The reduction in propanil adsorption in mesopores of BC after loading 300 μmol g⁻¹ of TA was 78% at both pHs. This reduction being larger than the 57% reduction in mesopore surface area suggests that loading TA made the mesopore surface less accessible to propanil, due presumably to the enhanced surface obstruction by TA and associated waters around the increased acidic groups.

In summary, BC in soils may exist as associates with natural organic matter as DOM can be strongly coated on the carbon surfaces. Due to the presence of an abundance of acidic groups in DOM, its coatings can increase the surface acidity and hence decrease the isoelectric point of BC. An enhanced pH influence on the adsorption of, for example, dissociable pesticides is thus expected. DOM coatings can also effectively block various pores of BC, rendering its surface partially inaccessible to pesticide molecules and hence reducing the pesticide adsorption. Considering that DOM is composed of a spectrum of molecules differing widely in molecular size, selective coatings and pore blocking can occur thereby resulting in a size-dependent influence on the pesticide adsorption. From our results, it is expected that humic acid would create a much stronger influence than fulvic acid on the adsorption of pesticides by BC. These predictions have been verified in this study by loading organic acids of different molecular sizes onto a BC and subsequently determining the adsorption of pesticides with different protonation and deprotonation properties. It is thus clear that DOM must be taken into consideration in evaluating the role of BC in the environmental fate of pesticides.

Supporting Information Available

HPLC chromatograms of tannic acid, gallic acid and propanil. Tannic acid and gallic acid adsorption isotherms on BC and their Freundlich parameters. Zeta potentials of BC samples.

Freundlich parameters for pesticide adsorption isotherms. Adsorption of pesticides by BC at the equilibrium concentration of 30 mg/L. This material is available free of charge via the Internet at http://pubs.acs.org.

Literature Cited

(1) Koelmans, A. A.; Jonker, M. T. O.; Cornelissen, G.; Bucheli, T. D.; Van Noort, P. C. M.; Gustafsson, Ö. Black carbon: The reverse of its dark side. *Chemosphere* **2006**, *63*, 365–377.

(2) Masiello, C. A.; Druffel, E. R. M. Black carbon in deep-sea sediments. *Science* **1998**, *280*, 1911–1913.

(3) Crutzen, P. J.; Andreae, M. O. Biomass burning in the tropics: Impact on atmospheric chemistry and biogeochemical cycles. *Science* **1990**, *250*, 1669–1678.

(4) Yang, Y.; Sheng, G. Enhanced pesticide sorption by soils containing particulate matter from crop residue burns. *Environ. Sci. Technol.* **2003**, *37*, 3635–3639.

(5) Cornelissen, G.; Gustafsson, Ö.; Bucheli, T. D.; Jonker, M. T. O.; Koelmans, A. A.; Noort, P. C. M. V. Extensive sorption of organic compounds to black carbon, coal, and kerogen in sediments and soils: Mechanisms and consequences for distribution, bioaccumulation, and biodegradation. *Environ. Sci. Technol.* **2005**, *39*, 6881–6895.

(6) Sheng, G.; Yang, Y.; Huang, M.; Yang, K. Influence of pH on pesticide sorption by soil containing wheat residue-derived char. *Environ. Pollut.* **2005**, *134*, 457–463.

(7) Jonker, M. T. O.; Koelmans, A. A. Sorption of polycyclic aromatic hydrocarbons and polychlorinated biphenyls to soot and soot-like materials in the aqueous environment: Mechanistic considerations. *Environ. Sci. Technol.* **2002**, *36*, 3725–3734.

(8) Zhang, P.; Sheng, G.; Feng, Y.; Miller, D. M. Role of wheat-residue-derived char in the biodegradation of benzonitrile in soil: Nutritional stimulation versus adsorptive inhibition. *Environ. Sci. Technol.* **2005**, *39*, 5442–5448.

(9) Chun, Y.; Sheng, G.; Chiou, C. T.; Xing, B. Compositions and sorptive properties of crop residue-derived chars. *Environ. Sci. Technol.* **2004**, *38*, 4649–4655.

(10) Yang, Y.; Chun, Y.; Sheng, G.; Huang, M. pH-Dependence of pesticide adsorption by wheat-residue-derived black carbon. *Langmuir* **2004**, *20*, 6736–6741.

(11) Qiu, Y. P.; Cheng, H. Y.; Xu, C.; Sheng, G. D. Surface characteristics of crop-residue-derived black carbon and lead (II) adsorption. *Water Res.* **2008**, *42*, 567–574.

(12) Cornelissen, G.; Gustafsson, Ö. Sorption of phenanthrene to environmental black carbon in sediment with and without organic matter and native sorbates. *Environ. Sci. Technol.* **2004**, *38*, 148–155.

(13) Pignatello, J. J.; Kwon, S.; Lu, Y. Effect of natural organic substances on the surface and adsorptive properties of environmental black carbon (char) attenuation of surface activity by humic and fulvic acids. *Environ. Sci. Technol.* **2006**, *40*, 7757–7763.

(14) Wang, G. S.; Alben, K. T. Effect of preadsorbed background organic matter on granular activated carbon adsorption of atrazine. *Sci. Total Environ.* **1998**, *224*, 221–226.

(15) Yang, Y.; Sheng, G. Pesticide adsorptivity of aged particulate matter arising from crop residue burns. *J. Agric. Food Chem.* **2003**, *51*, 5047–5051.

(16) Cornelissen, G.; Gustafsson, Ö. Effects of added PAHs and precipitated humic acid coatings on phenanthrene sorption to environmental black carbon. *Environ. Pollut.* **2006**, *141*, 526–531.

(17) McDonough, M. K.; Fairey, J. L.; Lowry, G. V. Adsorption of polychlorinated biphenyls to activated carbon: Equilibrium isotherms and a preliminary assessment of the effect of dissolved organic matter and biofilm loadings. *Water Res.* **2007**, *42*, 575–584.

(18) Matsui, Y.; Fukuda, Y.; Inoue, T.; Matsushita, T. Effect of natural organic matter on powdered activated carbon adsorption of trace contaminants: Characteristics and mechanism of competitive adsorption. *Water Res.* **2003**, *37*, 4413–4424.

(19) Li, F. S.; Yuasa, A.; Ebie, K.; Azuma, Y.; Hagishita, T.; Matsui, Y. Factors affecting the adsorption capacity of dissolved organic matter onto activated carbon: modified isotherm analysis. *Water Res.* **2002**, *36*, 4592–4604.

(20) Li, Q. L.; Snoeyink, V. L.; Mariñas, B. J.; Campos, C. Pore blockage effect of NOM on atrazine adsorption kinetics of PAC: The roles of PAC pore size distribution and NOM molecular weight. *Water Res.* **2003**, *37*, 4863–4872.

(21) Kilduff, J. E.; Wigton, A. Sorption of TCE by humic-preloaded activated carbon incorporating size-exclusion and pore blockage phenomena in a competitive adsorption model. *Environ. Sci. Technol.* **1999**, *33*, 250–256.

(22) Carter, M. C.; Weber, W. J., Jr.; Olmstead, K. P. Effects of background dissolved organic matter on TCE adsorption by GAC. *J. Am. Water Works Assoc.* **1992**, *84*, 81–91.

(23) Guo, Y. P.; Yadav, A.; Karanfil, T. Approaches to mitigate the impact of dissolved organic matter on the adsorption of synthetic organic contaminants by porous carbonaceous sorbents. *Environ. Sci. Technol.* **2007**, *41*, 7888–7894.

(24) Pignatello, J. J.; Lu, Y.; LeBoeuf, E. J.; Huang, W.; Song, J.; Xing, B. Nonlinear and competitive sorption of apolar compounds in black carbon-free natural organic materials. *J. Environ. Qual.* **2006**, *35*, 1049–1059.

(25) Hedges, J. I. Polymerization of humic substances in natural environments. In *Humic Substances and Their Role in the Environment*; Frimmel, F. H. Christman, R. F., Eds., Wiley: New York, 1988.

(26) Howard, P. H.; Meylan, W. M. *Handbook of Physical Properties of Organic Chemicals*; Lewis Publishers: Boca Raton, FL, 1997.

(27) Mueller-Harvey, I.; Mlambo, V.; Sikosana, J. L. N.; Smith, T.; Owen, E.; Brown, R. H. Octanol-water partition coefficients for predicting the effects of tannins in ruminant nutrition. *J. Agric. Food Chem.* **2007**, *55*, 5436–5444.

(28) Montgomery, J. J. *Agrochemicals Desk Reference*, 2nd ed.; Lewis Publishers: Boca Raton, FL, 1997.

(29) Barrett, E. P.; Joyner, L. G.; Halenda, P. P. The determination of pore volume and area distributions in porous substances: I. Computations from nitrogen isotherms. *J. Am. Chem. Soc.* **1951**, *73*, 373–380.

(30) Horvath, G.; Kawazoe, K. Method for the calculation of effective pore size distribution in molecular sieve carbon. *J. Chem. Eng. Jpn.* **1983**, *16*, 470–475.

(31) Boehm, H. P. Some aspects of the surface chemistry of carbon blacks and other carbons. *Carbon* **1994**, *32*, 759–769.

(32) Wang, X.; Yang, K.; Tao, S.; Xing, B. Sorption of aromatic organic contaminants by biopolymers: Effects of pH, copper (II) complexation, and cellulose coating. *Environ. Sci. Technol.* **2007**, *41*, 185–191.

(33) Goldberg, E. D. *Black Carbon in the Environment: Properties and Distribution*; John Wiley & Sons: New York, 1985.

(34) Mattson, J. S.; Mark, H. B. *Activated Carbon: Surface Chemistry and Adsorption from Solution*; Marcel Dekker: New York, 1971.

(35) Jung, M. W.; Ahn, K. H.; Lee, Y. H.; Kim, K. P.; Rhee, J. S.; Park, J. T.; Paeng, K. J. Adsorption characteristics of phenol and chlorophenols on granular activated carbons (GAC). *Microchem. J.* **2001**, *70*, 123–131.

(36) Wang, X.; Xing, B. Sorption of organic contaminants by biopolymer-derived chars. *Environ. Sci. Technol.* **2007**, *41*, 8342–8348.

(37) Zhu, D. Q.; Pignatello, J. J. Characterization of aromatic compound sorptive interactions with black carbon (charcoal) assisted by graphite as a model. *Environ. Sci. Technol.* **2005**, *39*, 2033–2041.

(38) Zhu, D. Q.; Kwon, S.; Pignatello, J. J. Adsorption of single-ring organic compounds to wood charcoals prepared under different thermochemical conditions. *Environ. Sci. Technol.* **2005**, *39*, 3990–3998.

(39) Pelekani, C.; Snoeyink, V. L. Competitive adsorption between atrazine and methylene blue on activated carbon: The importance of pore size distribution. *Carbon* **2000**, *38*, 1423–1436.

(40) Pelekani, C.; Snoeyink, V. L. Competitive adsorption in natural water: Role of activated carbon pore size. *Water Res.* **1999**, *33*, 1209–1219.

(41) Hsieh, C. T.; Teng, H. Influence of mesopore volume and adsorbate size on adsorption capacities of activated carbons in aqueous solutions. *Carbon* **2000**, *38*, 863–869.

(42) Frisch, M. J.; Trucks, G. W.; Schlegel, H. B.; et al. *Gaussian 98, Revision A.3*; Gaussian Inc.: Pittsburgh, PA, 1998.

(43) Grebennikov, S. F.; Serpinskii, V. V.; Pakhomov, Y. I.; Yakubov, T. S. Mechanism of bulk micropore filling in charcoal adsorbents. *Russ. Chem. B.* **1983**, *3*, 498–503.

(44) Gregg, S. J.; Sing, K. S. W. *Adsorption, Surface Area and Porosity*; Academic Press: London, 1982.